

Immuno informatics Approach in Designing a Novel Vaccine Using Epitopes from All the Structural Proteins of SARS-CoV-2

Leana Rich M. Herrera

Department of Physical Sciences, College of Science,
Polytechnic University of the Philippines, Manila City, Philippines.

*Corresponding Author E-mail: lrmherrera@pup.edu.ph

<https://dx.doi.org/10.13005/bpj/2060>

(Received: 02 August 2020; accepted: 31 October 2020)

The rapid transmission of severe acute respiratory syndrome coronavirus 2 (SARS-CoV-2) has resulted to the death of hundreds of thousands of people worldwide. With the devastating effects on the economy and healthcare system of many countries, it is crucial to accelerate vaccine development against SARS-CoV-2. Thus, this work utilized immuno informatics to efficiently design a novel multi-epitope vaccine that can potentially induce immune response through the immunogenic, and abundantly expressed structural proteins in SARS-CoV-2. Epitopes were screened and evaluated using various immuno informatics tools and databases. Antigenicity, allergenicity, and population coverage were assessed. Epitopes were adjoined to form a single vaccine construct (Covax), linked with 50S ribosomal protein as an adjuvant. Physicochemical properties, cross-reactivity, antigenicity, and allergenicity of Covax were evaluated. The tertiary structure of Covax was modeled, refined and validated for docking with toll-like receptor 4 (TLR4). Binding affinity of Covax-TLR4 was estimated and compared with TLR4-adjuvant as control. Lastly, the immune response with Covax was simulated and compared with adjuvant alone. Total of 33 epitopes from S (21), E (3), M (5), and N (4) proteins were merged in Covax. These include epitopes on the receptor-binding motif (RBM) of S protein known to be essential in the viral attachment. In silico evaluations classified Covax as stable, antigenic, and non-allergenic. Epitopes were estimated to have large worldwide population coverage, especially in areas with high infection rates, indicating broad potential efficacy of Covax as a vaccine for the most affected populations. Results in this work showed that Covax can bind to TLR4 which indicates potential immunogenicity and superior properties necessary for a successful vaccine. Overall, this work efficiently minimized time, effort and cost in designing a candidate vaccine against SARS-CoV-2. In vitro and in vivo studies on Covax are anticipated.

Keywords: Epitopes, immuno informatics, in silico, receptor-binding motif, SARS-CoV-2, vaccine.

The coronavirus disease 2019 (COVID-19) pandemic is caused by the severe acute respiratory syndrome coronavirus 2 (SARS-CoV-2) outbreak which was first identified in Wuhan, China in December 2019 (Li Q *et al.*, 2020). This novel virus attacks vital organs, mainly the lungs which can progress into fatal pneumonia and acute respiratory distress syndrome (Wang *et al.*, 2020). SARS-CoV-2 can be easily transmitted through

direct contact, fomites, and respiratory droplets (Galbadage, *et al.*, 2020). However, infected individuals may or may not have symptoms which commonly include fever, cough, and fatigue (Huang *et al.*, 2020). Since SARS-CoV-2 has just been discovered recently, very little is known about its pathogenesis. Further investigative studies on the nature of this novel virus must be conducted.



Currently known human corona viruses (HCoV) including HCoV-229E and HCoV-NL63 belong to genus *Alpha coronavirus* while HCoV-OC43, HCoV-HKU1, Middle East Respiratory Syndrome (MERS), SARS-CoV and SARS-CoV-2 belong to genus *Beta coronavirus*, family *Coronaviridae* (Al-Tawfiq *et al.*, 2014). Phylogenetic studies showed SARS-CoV-2 shared 96% and 79.6% sequence identity with bat coronavirus and SARS-CoV, respectively (Zhou *et al.*, 2020). Coronaviruses are enveloped viruses containing positive sense single-stranded RNA as genetic material. It has approximately 26-30 kb encoding non-structural proteins (NSP) and structural proteins including spike (S), envelope (E), membrane (M) and nucleocapsid (N) (Ahmed SF, *et al.*, 2020). Structural proteins in coronaviruses have different roles yet with integrative functions. Glycosylated S protein consists of two subunits S1 and S2 forming a trimeric structure on the surface of the virus similar to spikes of a crown (Walls *et al.*, 2016). S protein is vital in cell host attachment, fusion, and entry. It contains a receptor-binding motif (RBM) which binds with angiotensin-converting enzyme 2 (ACE2) receptor of the host cell facilitating its entry (Hoffmann *et al.*, 2020). These crucial roles make S protein the most valuable target in vaccines and therapeutics (Zhu *et al.*, 2013). Coronavirus E protein is a single-pass transmembrane protein which self-assembles in host membrane acting as a viroporin to allow the transport of ions (Verdia-Baguena *et al.*, 2013; Wilson *et al.*, 2004). It is the smallest structural protein in coronaviruses yet plays important roles in assembly, viral release, and contributes in the virulence of HCoVs (Nieto-Torres *et al.*, 2014). N protein is the only structural protein known to bind and encapsidate the genomic RNA (gRNA) of coronaviruses (Ma *et al.*, 2010; Kuo *et al.*, 2016). It is also abundantly expressed in the host cell during infection making it an excellent target in constructing vaccines to induce activation of cytotoxic (CTL) and helper T lymphocytes (HTL). This multi-functional protein plays important roles in organization of viral particles through its association with gRNA and with M protein (McBride *et al.*, 2014). M protein is a small transmembrane protein integrated in the membrane of all coronaviruses. Its participation for intracellular viral assembly

is S protein-dependent. As the most abundant structural protein in corona viruses, M protein is also involved in packaging gRNA, regulation of replication, and morphogenesis (Neuman BW, *et al.*, 2010; Hu Y, *et al.*, 2003). A recent study showed that T-cell responses elicited by SARS-CoV structural proteins are more immunogenic than the nonstructural proteins (Li *et al.*, 2008). Since the genetic sequence of SARS-CoV-2 shares a close identity with SARS-CoV, generating epitopes from the sequences of these structural proteins is a good strategy to develop an immunotherapeutic agent against COVID-19.

SARS-CoV-2 pandemic warrants urgent discovery of anti-viral drugs and vaccines. Immuno informatics and data mining have efficiently hastened and reduced the cost required in experimental immunology to identify vaccine candidates and biomarkers (Vaishnav *et al.*, 2015; Oyarzún *et al.*, 2016). Just to mention a few, immuno informatics has aided in designing vaccines that demonstrated safety, and promising results against herpes simplex virus type 2 and human influenza H1N1, both of which are currently under preclinical and clinical trials, respectively (Pan *et al.*, 2012; Pleguezuelos *et al.*, 2020). Thus, the primary goal of this work is to apply immuno informatics tools, and databases to efficiently design a vaccine that can potentially induce immune response against SARS-CoV-2. Several vaccine candidates against SARS-CoV-2 are already in clinical trials; however, these cannot guarantee success—the pursuit for a safe and effective vaccine is far from being resolved. This work focused in designing a multi-epitope vaccine from all the structural proteins of SARS-CoV-2. Constructing a multi-epitope vaccine could be more advantageous than single peptides. These include larger population coverage, simultaneous induction of immune response due to the adjoined promiscuous epitopes, linkage of an adjuvant which increases immunogenicity of the epitopes, and exclusion of sequences that can result to adverse effects.

METHODOLOGY

Retrieval of Sequences

Thirty three SARS-CoV-2 isolates from different areas around the world including

Taiwan, Turkey, Sweden, Iran, Brazil, Australia, Bangladesh, Columbia, Czechoslovakia, France, Greece, India, Peru, Serbia, South Africa, Spain, China, Germany, Guam, Hong Kong, Israel, Italy, Kazakhstan, Malaysia, Nepal, Pakistan, Puerto Rico, Korea, Sri Lanka, Thailand, California USA, Uruguay, and Vietnam were retrieved in the NCBI Virus database (date retrieved: June 1, 2020). Only those with complete sequences were retrieved, and environmental sources were excluded. The S, E, M, and N protein sequences from these isolates which are accessible in supplementary file 1 (Supp1), were aligned per protein using Clustal Omega. To identify conserved fragments, protein variability analysis was conducted in Protein Variability Server using Shannon entropy threshold of 1.0 (Shannon 1948). Resulting conserved sequences were used for the screening of epitopes. In addition, the amino acid sequences of S, E, M, and N proteins from HCoV-229E, MERS, HCoV-HKU1, HCoV-OC43, SARS-CoV, and SARS-CoV-2 (NC_002645.1, NC_019843.3, NC_006577.2, NC_006213.1, NC_004718.3, and NC_045512.2) were also retrieved from the National Center for Biotechnology Information (NCBI) for cross-reactivity analysis.

Identification of Linear B Lymphocyte (BL) Epitopes

The positions of extraviroin sequences for SARS-CoV-2S protein (13-1213), E protein (1-16), and M protein (2-19) are fully annotated in the UniProt database. These extraviroin sequences were used to screen for linear B lymphocyte (BL) epitopes. N protein doesn't have extraviroin sequences; thus, it was not included in BL epitope screening. Default parameters in Emini Surface Accessibility (ESA), BepiPred Linear Epitope (BLE), Kolaskar & Tongaonkar Antigenicity (KTA) tools in Immune Epitope Database (IEDB), and ABCPred Server were used to generate the best linear BL epitopes. Surface accessibility is an important factor to consider in predicting potent epitopes. ESA scale estimates the accessibility of a hexapeptide sequence and calculates a score indicating its probability to be found on the surface (Emini *et al.*, 1985). BLE prediction tool utilizes the combination of hidden Markov model and propensity scale method wherein the residues with scores above a certain threshold are presaged as epitopes (Jespersen *et al.*, 2017). KTA predicts

potential epitopes through amino acid residues and the frequency of their occurrence as epitopes based from experimental data. As applied to a large number of proteins, this tool was validated by Kolaskar and Tongaonkar (1990) to be 75% accurate, making it superior than other known methods in predicting epitopes. ABCPred uses artificial neural network and predicts BL epitopes with 65.93% accuracy (Saha & Raghava, 2006). Epitopes which overlapped with glycosylation and cleavage sites were excluded. Consensus BL epitopes with 12-15 residues from at least 2 servers were saved for further evaluations.

Identification of Helper T Lymphocyte (HTL) Epitopes

The complete amino acid sequence of S, E, M and N proteins from SARS-CoV-2 were used to screen for helper T lymphocyte (HTL) epitopes. HTL epitopes and their binding affinity with MHC II alleles were identified using NetMHCIIpan-3.2 in IEDB server. This method was built on an extended data set of quantitative MHC-peptide binding affinity which has improved the performance of peptide binding prediction (Jensen KK, *et al.*, 2018). HTL epitopes were obtained in this tool using the most frequent MHC II alleles (Greenbaum *et al.*, 2011), and $IC_{50} < 500 \text{ nmol/dm}^3$ which classifies epitopes as good binders (Jensen *et al.*, 2018). Resulting epitopes with 11 residues binding to almost all MHC II alleles from the list were saved for further evaluations. The list of the most frequent MHC II alleles used in the study can be accessed in supplementary file 2 (Supp2).

Identification of Cytotoxic T Lymphocyte (CTL) Epitopes

Complete amino acid sequence of S, E, M and N proteins from SARS-CoV-2 were screened for epitopes binding with the most frequent MHC I alleles (Weiskopf *et al.*, 2012) (Supp2). IEDB Proteasomal cleavage/transporter associated with antigen processing transport (TAP)/MHC class I combined predictor tool which employs NetMHCpan-2.0 method was utilized; thereby, considering proteasomal processing, TAP transport, and binding affinity in predicting CTL epitopes altogether. NetMHCpan-2.0 is trained using the broadest set of available MHC I binding data which can be used for large out-bred populations (Hoof *et al.*, 2009). Peptides with 9-11 residues, $IC_{50} < 500 \text{ nmol/dm}^3$, proteasome-processing score > 1.0 ,

TAP score > 1.0, and those which cover most of the frequent MHC I alleles were saved for further evaluations.

Evaluation of Predicted Epitopes

Predicted epitopes were further evaluated for antigenicity, allergenicity, cross-reactivity, % conservancy, and cross-protection. Antigenic epitopes were identified using threshold e^{-3} 0.5 in Vaxijen 2.0 Server with a virus as a target. Vaxijen is an alignment-independent method which predicts antigen based on the physicochemical properties of proteins with 70% to 89% accuracy (Doytchinova & Flower, 2007). Potential allergenic sites were assessed using Allergen FP v 1.0. The highest Tanimoto similarity index of an epitope matching an allergen sequence from the database is used to determine if the epitope is a probable allergen (Dimitrov *et al.*, 2014). To avoid potential autoimmune reactions, predicted epitopes were queried for possible hits against human protein sequences in UniProtKB and SwissProt databases using default parameters in protein-protein BLAST (BLASTp). Possible cross-protection offered by each epitope against 6 other HCoV strains was also investigated in IEDB Conservancy Analysis Tool (IEDB-CAT). Predicted epitopes which passed all these evaluations were selected for inclusion in the vaccine.

Estimation of Population Coverage

The use of multi-epitopes could have larger population coverage (PC) for a vaccine. In this work, worldwide human PC were estimated using the Population Coverage tool in IEDB. The PC was calculated from each set of HTL and CTL epitopes as the vaccine will consist of multi-epitopes. In addition, PC in areas where infection rates of SARS-CoV-2 are high (North

America, Europe, East and Northeast Asia) were also estimated. This tool efficiently maximizes the population coverage of epitopes while minimizing the number of epitopes that must be included in a vaccine (Bui *et al.*, 2006).

Construction of the Multi-Epitope Vaccine

An adjuvant and the selected BL, HTL, and CTL epitopes from S, E, M and N proteins of SARS-CoV-2 were included in the vaccine—Covax. Overlapping CTL and HTL epitopes for the same protein were shortlisted using BL epitopes as template. For overlapping CTL and HTL epitopes which do not overlap with any BL epitopes, CTL epitopes were shortlisted using HTL epitopes as template. Within the same type of lymphocytes, overlapping epitopes for each protein were also merged as continuous peptides. To form the multi-epitope construct, BL and HTL epitopes were adjoined together using GPGPG linkers while CTL epitopes were adjoined using AAY linkers. For each type of lymphocyte, peptides from the same protein are arranged next to each other according to their positions in their respective proteins. For the adjuvant, sequence of 50S ribosomal protein (50S RP) from *Mycobacterium tuberculosis* strain ATCC 25618/H37Rv (UniProt ID: P9WHE3) was linked with the N-terminus of the multi-epitope construct via flexible alpha-helix-forming EAAAK linker. In the complete Covax construct, adjuvant is followed by each set of CTL, then HTL, and lastly BL peptides at the end to make it more accessible. Finally, Valine was added at the N-terminus of the vaccine construct to increase its half-life.

Evaluation of Physicochemical Properties, Antigenicity, Allergenicity, and Cross-Reactivity of Covax

The cross-reactivity of the candidate

Table 1. Selected BL epitopes

Epitope	Antigen	Antigenicity score	Length	Position
GTTLDSKTQSLIV	S	0.8614	14	107-120
GAAAYYVGYLQPRT	S	0.9243	14	261-274
AVDCALDPLSETKC	S	0.8534	14	288-301
GIYQTSNFRVQPT	S	1.0038	14	311-324
GKIADYNYKLPDDF	S	0.9776	14	416-429
GFNCYFPLQSYGFQ	S	0.8237	14	485-498
YGFQPTNGVGYQ	S	0.7136	12	495-506
DQLTPTWRVYSTGS	S	0.7635	14	627-640
LSSTASALGKLQDV	S	0.8753	14	938-951

vaccine against proteins expressed in humans was investigated using default parameters in BLASTp. Models, non-redundant refseq proteins, and uncultured environmental samples were excluded. Allergenicity and antigenicity of the candidate vaccine were further assessed in AllergenFP v1.1 and Vaxijen 2.0 servers, respectively. Molecular weight, amino acid composition, isoelectric point (pI), half-life, extinction coefficient, instability index, thermostability (aliphatic index) and grand average hydropathicity (GRAVY) of Covax were calculated using ProtParam tool in ExPASy server.

Secondary Structure and Tertiary Structure Modelling

Percentage composition of secondary structures in Covax was estimated using GOR4 web tool. Intrinsically disordered regions were determined using GlobPlot2v2.3 server. Tertiary structures of Covax and 50S RP were modelled using Galaxy TBM tool. This tool employs multiple-template approach and ab initio modelling, evaluated to be one of the top TBM servers (Ko *et al.*, 2012). Human toll-like receptor 4 (TLR4) crystal structure (PDB ID: 4G8A) was also retrieved. The ligands from the PDB structure were removed and only the monomeric form of TLR4 was used. The initial tertiary structure models of Covax, 50S RP, and retrieved crystal structure of human TLR4 were further refined in Galaxy Refine server. To check the validity of refined structures, ERRAT, Verify3D, and Rampage servers were employed. ERRAT analyzes the nonbonded atom to atom interactions of the input structure as compared with crystallography structures (Colovos & Yeates,

1993). Verify3D measures the compatibility of the tertiary structure model with its protein sequence which is then compared with the results of good structures (Eisenberg *et al.*, 1997). Rampage generated Ramachandran plots showing the percentage of residues lying within the favoured, allowed, and disallowed regions. The best refined tertiary structure models were viewed in Pymol and were used for protein-protein docking. Covax was further investigated for structural BL epitopes.

Identification of Structural B-Cell Epitopes

BL epitopes incorporated in Covax must be accessible and protruded enough so B-cell receptors (BCRs) can bind to it. Ellipro was utilized in the study to identify structural epitopes on the tertiary structure model of Covax. To date, it is the best structure-based algorithm amongst the others (Ponomorenko, *et al.*, 2008). It predicts conformational and linear BL epitopes based from protrusion index (PI) of a residue, and provides PI score for each protruded sequence.

Molecular Docking Interaction of Covax-TLR4 and Peptide-HLA

An antigen must bind to specific immune receptor to elicit an immune response. Thus, this work conducted data-driven docking to assess possible interactions between Covax containing 50S RP as its adjuvant, with the human TLR4 using Clus Proserver. This tool performs rigid docking based on Fast Fourier Transform by conducting conformation sampling, complex pair-wise root-mean-square deviation, and energy minimization step to yield docked complexes together with their calculated binding energy scores (Kozakov

Table 2. Selected HTL epitopes

Epitope	Antigen	Antigenicity Score	Position
LPFFSNVTWFH	S	0.7486	56-66
PFFSNVTWFHA	S	0.584	57-67
SLLVNNATNV	S	0.5504	116-126
TLLALHRSYLT	S	0.5459	240-250
LLALHRSYLT	S	0.7771	241-251
NFRVQPTESIV	S	1.0669	317-327
IPFAMQMAYRF	S	1.2909	896-906
VTLAILTALRL	E	0.8965	29-39
SFRLFARTRSM	M	0.5944	99-109
IGAVILRGHLR	M	0.8668	140-150
PANNAIIVLQL	N	0.6257	151-161
ALLLDRLNQL	N	0.5127	220-230

et al., 2017). In this study, the best complex pose in terms of the lowest energy and docking positions was chosen and viewed in Pymol. The tertiary structure models for 50S RP and TLR4 were also docked and was utilized as control. The binding affinities and contact interfaces of docked structures at 37 °C were evaluated in PRODIGY web server which uses intermolecular contacts and non-interface surface properties for predictive models (Xue LC, *et al.*, 2016). Binding affinity and binding energy of Covax-TLR4 complex were compared with adjuvant-TLR4 complex. Common residues between the candidate vaccine and the lone adjuvant that are involved in the interaction with human TLR4 were investigated. The crystal structures of HLA-B*53:01 (PDB ID: 1A1M) and HLA-DRB1*04:05 (PDB ID: 4IS6) were retrieved from RCSB database. Galaxy WEBPep Dock server was utilized to dock the cleaned structures of HLA-B*53:01 and HLA-DRB1*04:05 with two the epitopes having the lowest binding affinity (highest IC50) from each set of selected CTL (FARTRSMWSF) and HTL (TLLALHRSYLT) epitopes resulted in this work. Docked structures were refined in Galaxy WEB Refine Complex server. Binding energy and binding affinity were calculated in PRODIGY web server.

Immune Simulation

The immunogenicity of Covax was further evaluated in silico using the C-ImmSim server. This simulates the cellular and humoral responses of the immune system against an amino

acid sequence (Rapin *et al.*, 2010). This tool has been previously used to model Epstein–Barr virus (Castiglione *et al.* 2007a) and HIV infection (Baldazzi *et al.* 2006; Castiglione *et al.* 2007b). Default simulation parameters were used in this study for a prophylactic vaccine injected three times in four weeks intervals (time steps set at 1, 84, and 168) with 200simulation steps. The immune response profile of Covax was compared with that of the adjuvant alone.

In Silico Cloning Optimization of Covax

For the efficient cloning of Covax in E.coli K12 strain, in silico codon optimization was conducted using Java Codon Adaptation Tool (JCAT). This tool calculates for the Codon Adaptation Index (CAI) to approximate the efficiency of gene expression with respect to the subset of highly expressed genes in an organism. The closer the CAI-value to 1, the more a gene will be highly expressed in a host (Grote *et al.*, 2005). GC-content of the candidate vaccine was also calculated.

RESULTS

Identification of Conserved Fragments in S, E, M and N Proteins

Using Shannon entropy threshold < 1.0, the protein variability analysis for retrieved S, E, M, and N sequences generated conserved amino acid sequences(Supp3) for each structural protein which were then used to predict SARS-CoV-2 epitopes.

Table 3. Selected CTL Epitopes

Epitope (residues)	Antigen	Antigenicity score	Position	Proteosome-processing score	TAP score
GWTAGAAAYY (10)	S	0.5358	257-266	1.24	1.31
WTAGAAAYY (9)	S	0.6306	258-266	1.24	1.24
YYVGYLQPRTF (11)	S	0.8985	265-275	1.36	1.31
SETKCTLKSF (10)	S	0.6433	297-306	1.4	1.07
IPFAMQMAYRF (11)	S	1.2909	896-906	1.45	1
NVSLVKPSFY (10)	E	0.7279	48-57	1.19	1.36
VSLVKPSFYVY (11)	E	0.616	49-59	1.51	1.38
QWNLVIGFLF (10)	M	1.2302	19-28	1.12	1.1
FARTRSMWSF (10)	M	0.9202	103-112	1.41	1.12
ATSRTLSTYY (9)	M	0.6108	171-179	1.26	1.34
KDLSRWYFY (11)	N	0.9184	102-112	1.07	1.21
AQFAPSASAF (10)	N	0.5986	305-314	1.23	1.25

Linear BL Epitopes in SARS-CoV-2

Predicted linear BL epitopes from the extraviroin sequences of S, E and M proteins yielded 1-24 residues. After further assessments, predicted epitopes from E and M proteins did not pass the antigenicity test in Vaxijen server. Only the S protein generated 9 BL epitopes (12-14 residues) which are all consensus sequences from at least 2 prediction tools. These are also antigenic, non-allergenic, and without significant matches in human proteins (Table 1).

HTL Epitopes in SARS-CoV-2

Table 2 shows the 12 selected HTL epitopes from S (7), E (1), M (2), and N (2) proteins. All have good binding affinity ($IC_{50} < 500 \text{ nmol/dm}^3$) with their respective human MHC II alleles (Supp4). Furthermore, these 12 epitopes are classified antigenic, non-allergenic, and without significant matches with human proteins in the databases. The world population coverage for the series of HTL epitopes in Covax is estimated to be 81.81%, while this set covers 85.83%, 81.82%, 59.99% and 87.89% of populations in Europe, East Asia, Northeast Asia, and North America, respectively. In addition, IPFAMQMAYRF, VTLAILTALRL,

SFRLFARTRSM and ALLLLDRLNQL from S, E, M, and N proteins, respectively, may offer cross-protection as they share 100% sequence identity with SARS-CoV besides COVID-19 (Supp5).

CTL Epitopes in SARS-CoV-2

Cytotoxic lymphocytes play vital roles against viral pathogens that infect and replicate inside the host cell. This work selected 12 CTL epitopes (9-11 residues) on S (5), E (2), M (4), and N (2) structural proteins of SARS-CoV-2 (Table 3). These epitopes have good binding affinities ($IC_{50} < 500 \text{ nmol/dm}^3$) with their respective human MHC I alleles (Supp6), as well as efficient proteasome processing and TAP scores (> 1.0). All 12 epitopes are antigenic, non-allergenic, and without significant matches across human proteins. Besides SARS-CoV-2, these epitopes may offer cross-protection against SARS-CoV as QWNLVIGFLF (M), FARTRSMWSF (M), AQFAPSASAF (N), and IPFAMQMAYRF (S) shared 100% sequence identity with SARS-CoV (Supp5). Moreover, the set of CTL epitopes largely covers 85.87% of world population while 80.17% of population is covered in Northeast Asia particularly China (80.1%), 85.18% in East Asia,

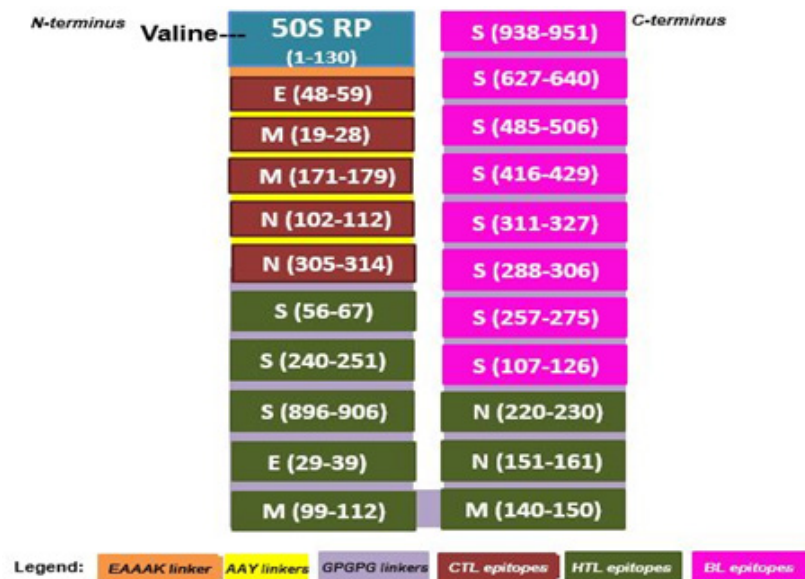


Fig. 1. Covax Multi-Epitope Construct. At the N-terminus of Covax, a Valine residue is bonded to the first residue of 50S RP adjuvant (blue). The adjuvant is linked to the first CTL epitope (maroon) via EAAAK linker (orange). The positions of each epitope based from the sequence of each structural protein is indicated in parenthesis. Five CTL peptide sequences (maroon) were adjoined via AAY linkers (yellow) while 8 HTL (olive green) and 8 BL peptide sequences (pink) were adjoined via GPGPG linkers (violet). BL peptides contain overlapping CTL and HTL epitopes as a result of merging. S, E, M, and N are the four structural antigens of SARS-CoV-2

90.78% in Europe, and 86.67% in North America including the U.S.A. with high infection rates of COVID-19.

Construction of Multi-Epitope Vaccine

Figure 1 shows a schematic presentation of Covax multi-epitope construct which consists of 510 residues. Herein, the overlapping sequences from the total of 33 selected epitopes generated in this work were merged to form 21 continuous fragments. Covax includes a Valine residue added at the N-terminus aiming to increase its half-life.

Properties of the Vaccine Candidate

Covax is classified as antigenic (0.5852) in Vaxijen server with virus as target, and is also a non-allergen having the highest Tanimoto similarity index of 0.9 with its nearest protein (UniProtKB ID: Q9P281). Blast P analysis of Covax showed that it has no significant similarity with any human proteins; thus, avoiding possible autoimmune reactions. Protparam tool calculated that Covax has a molecular weight of 53,005.45 g/mol, and pI of 7.73 which can be used for purification purposes

in isoelectric focusing. Its extinction coefficient is 68,885 M⁻¹ cm⁻¹ at 280 nm wavelength in water, and absorbance is 1.3 assuming all pairs of cysteine residues form cystines. The estimated half-life of Covax is 100 hours in mammalian reticulocytes *in vitro*, >20 hours in yeast *in vivo*, and > 10 hours *in vivo* in E.coli. The instability index is 26.93 which classifies Covax as stable (<40). In addition, an aliphatic index of 81.24 indicates thermal stability while the small positive value of its GRAVY (0.036) implies its very weak hydrophobicity.

Secondary Structure Composition and Disordered Regions in Covax

Figure 2 shows that majority of the secondary structures in Covax are random coils (purple), alpha helix (blue), and extended strands (red). The stretch of linear BL epitopes in Covax(337-510) are mostly random coils and extended strands. In line with these, GlobPlot2 server identified disordered regions in Covax at positions 326-342, 352-366, 375-391, 398-415, and 421-504 which are less likely to form stable folded

Table 4. Quality Indicators for Tertiary Structure Validation

Tertiary structures	ERRAT	Verify3D	Ramachandran plot (favored, allowed, outlier)
Covax initial	73.52 %	76.08 %	92.6%, 5.2%, 2.2%
Covax refined	80.36 %	81.57%	95.5%, 3.5%, 1.0%
50S RP initial	99.18 %	84.62 %	95.3%, 3.1%, 1.6%
50S RP refined	100 %	92.31 %	94.5%, 4.7%, 0.8%
TLR4 (PDB:4G8A)	85.07 %	96.86 %	94.4%, 5.1%, 0.5%
TLR4 refined	89.06 %	97.02 %	97.7%, 1.8%, 0.5%

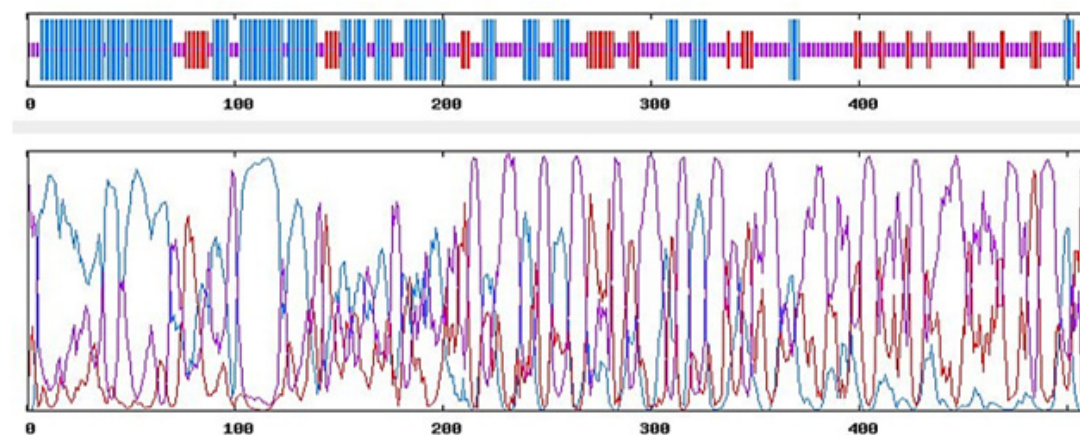


Fig. 2. Graphical representations of secondary structures in Covax. Predicted secondary structures in GOR4 include alpha helices (36.86%) in blue, extended strands (14.90%) in red, and random coils (48.24%) in purple

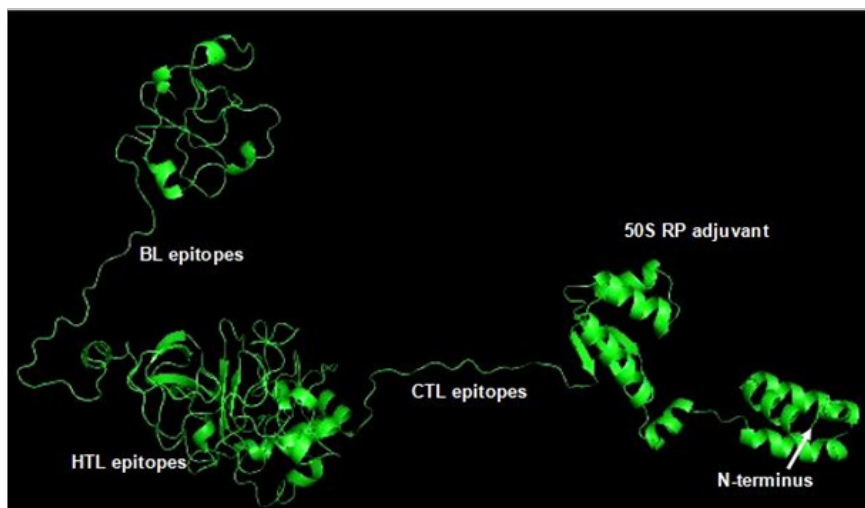


Fig. 3. Best tertiary structure model for Covax viewed inPymol

Table 5. Structural BL Epitopes in Covax.Linear and discontinuous structural BL epitopes which overlap with the series of SARS-CoV-2 BL epitopes are in bold text

Predicted epitopes	Sequence	Score	No. of residues
Linear	NATNVGPGPGGWTAGA (352-367)	0.644	16
	LKSFPGPGGGIYQT (401-414)	0.65	14
	ESIVGPGPGGKIADYNYKLPDDFGPGPGGFNCYFPLQSYGF QPTNGVGYQGPGPGDQLTPTWRVYSTGSGPGPLSSTASAL GKLQDV (423-510)	0.812	88
Discontinuous	A:L160, A:F161, A:Y164, A:A165, A:S167, A:R168, A:T169, A:L170, A:S171, A:Y172, A:Y173, A:A174, A:Y176, A:K177, A:H214, A:A215, A:G216, A:P217, A:G218, A:P219, A:G220, A:T221, A:Q243, A:M244, A:A245, A:Y246, A:A306, A:N307, A:N308, A:A309, A:A310, A:I311, A:V312, A:L313, A:Q314, A:L315, A:G316, A:P317, A:G318, A:P319, A:G320, A:A321, A:L322, A:L323, A:N351, A:N352, A:A353, A:T354, A:N355, A:V356, A:G357, A:P358, A:G359, A:P360, A:G361, A:G362, A:W363, A:T364, A:A365, A:G366, A:A367 A:E423, A:S424, A:I425, A:V426, A:G427, A:P428, A:G429, A:P430, A:G431, A:G432, A:K433, A:I434, A:A435, A:D436, A:Y437, A:N438, A:Y439, A:K440, A:L441, A:P442, A:D443, A:D444, A:F445, A:G446, A:P447, A:G448, A:P449, A:G450, A:G451, A:F452, A:N453, A:C454, A:Y455, A:F456, A:P457, A:L458, A:Q459, A:Y461, A:G462, A:F463, A:Q464, A:P465, A:T466, A:N467, A:G468, A:V469, A:G470, A:Y471, A:Q472, A:G473, A:P474, A:G475, A:P476, A:G477, A:D478, A:Q479, A:L480, A:T481, A:P482, A:T483, A:W484, A:R485, A:V486, A:Y487, A:S488, A:T489, A:G490, A:S491, A:G492, A:P493, A:G494, A:P495, A:G496, A:L497, A:S498, A:S499, A:T500, A:A501, A:S502, A:A503, A:L504, A:G505, A:K506, A:L507, A:Q508, A:D509, A:V510	0.561	61
		0.817	87

structure making these sequences more flexible for the binding of BCRs. Notice that most of the linear BL peptides in Covax(337-510) are within the disordered regions.

Prediction, Refinement and Validation of Tertiary Structures

By comparing the quality indicators, initial tertiary structure models of Covax, 50S RP and human TLR4 markedly improved after refinement (Table 4). Figure 3 shows the best tertiary structure model for Covax.

Structural B-Cell Epitopes of Covax

Ellipro revealed 3 linear and 2 discontinuous structural BL epitopes in the tertiary structure of Covax. These structural epitopes overlap with the series of SARS-CoV-2 BL epitopes (337-510) incorporated in the vaccine (Table 5).

Docking of Covax with Human TLR4 and HLA Molecules with Peptides

Figure 4 shows docked structures of the lowest interaction energy poses for 50SRP-TLR4 (Fig.4a) and Covax-TLR4 (Fig.4b). The estimated

binding energy (ΔG) and binding affinity (Kd) for are -41.42 KJ/mol and $1.0E-07$ mol/dm³ for 50SR-TLR4 complex, respectively. While the values are -38.49 KJ/mol and $3.4E-07$ mol/dm³ for Covax-TLR4. The number of interfacial contacts (IC) per property made at the interface of Covax-TLR4 (IC charged-charged: 20, IC charged-polar: 10, IC charged-apolar: 22, IC polar-polar: 1, IC polar-apolar: 2, IC apolar-apolar: 9) is higher than 50SRP-TLR4 (IC charged-charged: 19, IC charged-polar: 8, IC charged-apolar: 11, IC polar-polar: 5, IC polar-apolar: 11, IC apolar-apolar: 1). To further validate the protocols used in the selection of docked complexes, common interface residues between the two complexes were investigated. GLU16 of Covax and GLU15 of 50S RP both interact with LYS388 of TLR4. Other common interface residues interacting with TLR4 include GLU9, ALA13, THR18, GLU21 for Covax, and GLU8, ALA12, THR17, GLU20 for 50S RP. Figure 4 also shows that structures of HLA-DRB1*04:05-TLLALHRSYLT (Fig4c) and HLA-B*53:01-FARTRSMWSF (Fig.4d) fitted well on the binding

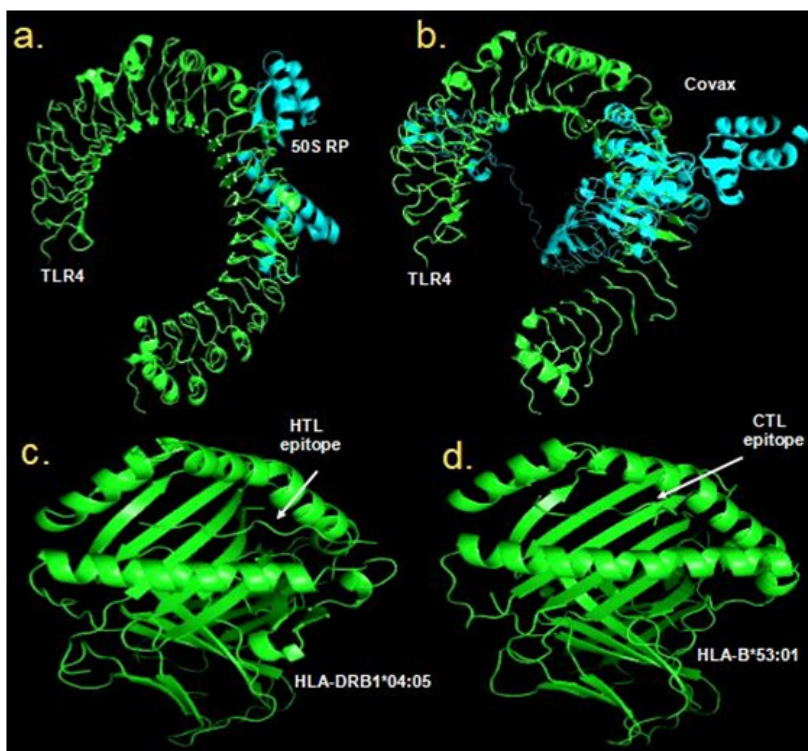
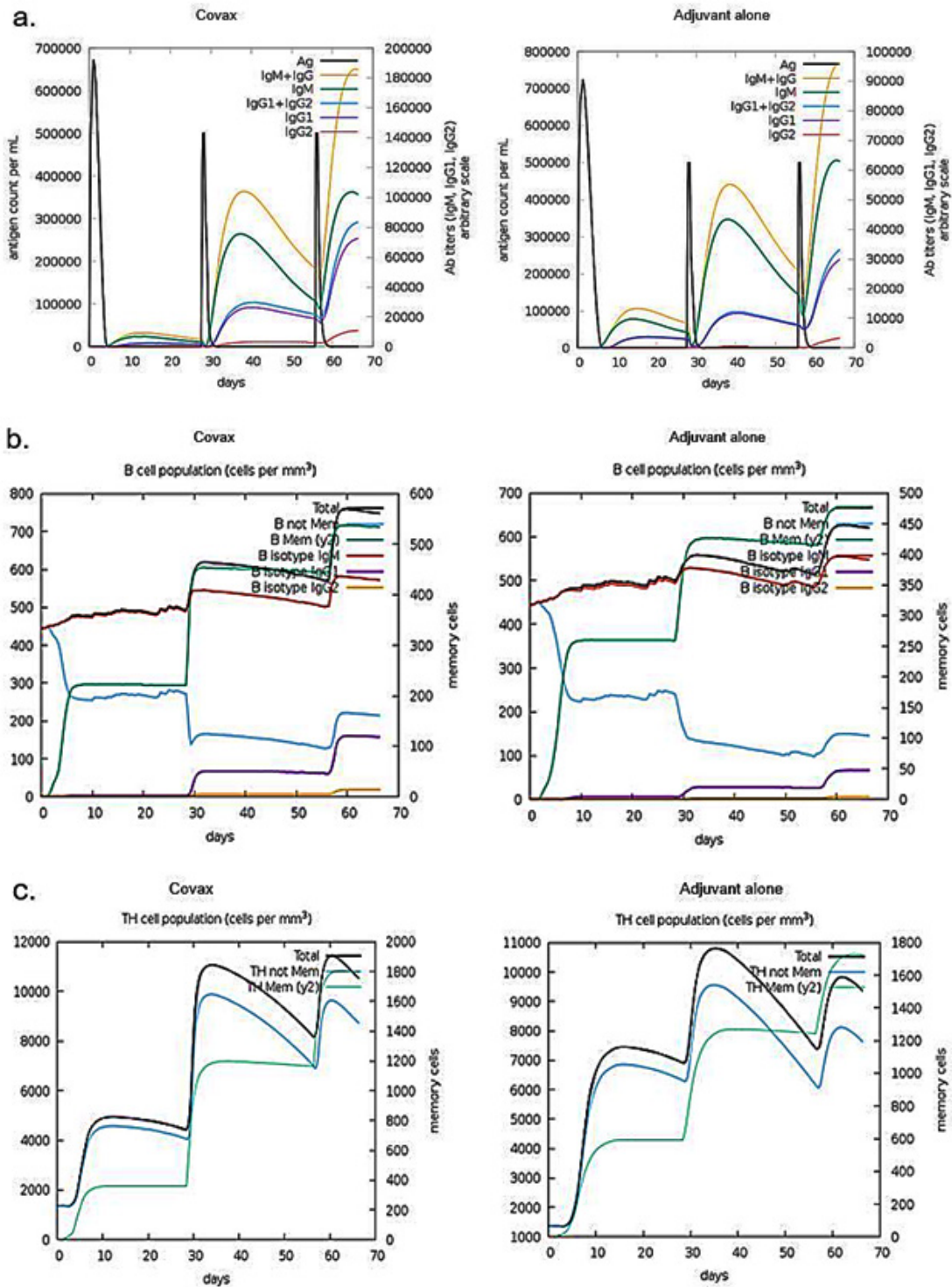


Fig. 4. Docking poses for complexes. ClusPro server generated top poses for 50SRP-TLR4 (a) and Covax-TLR4 (b); and GalaxyWEBPepdock server HTL epitope-HLA-DRB1*04:05 (c), and CTL epitope-HLA-B*53:01 (d) complexes

grooves. The binding energy and binding affinity for HLA-DRB1*04:05-TLLALHRSYLT are -49.37 KJ/mol and $5.1E-09$ mol/dm³, respectively. While the binding energy and binding affinity for

HLA-B*53:01-FARTRSMWSF are -36.40 KJ/mol and $6.9E-07$ mol/dm³, respectively.

Immune Response Profile of Covax



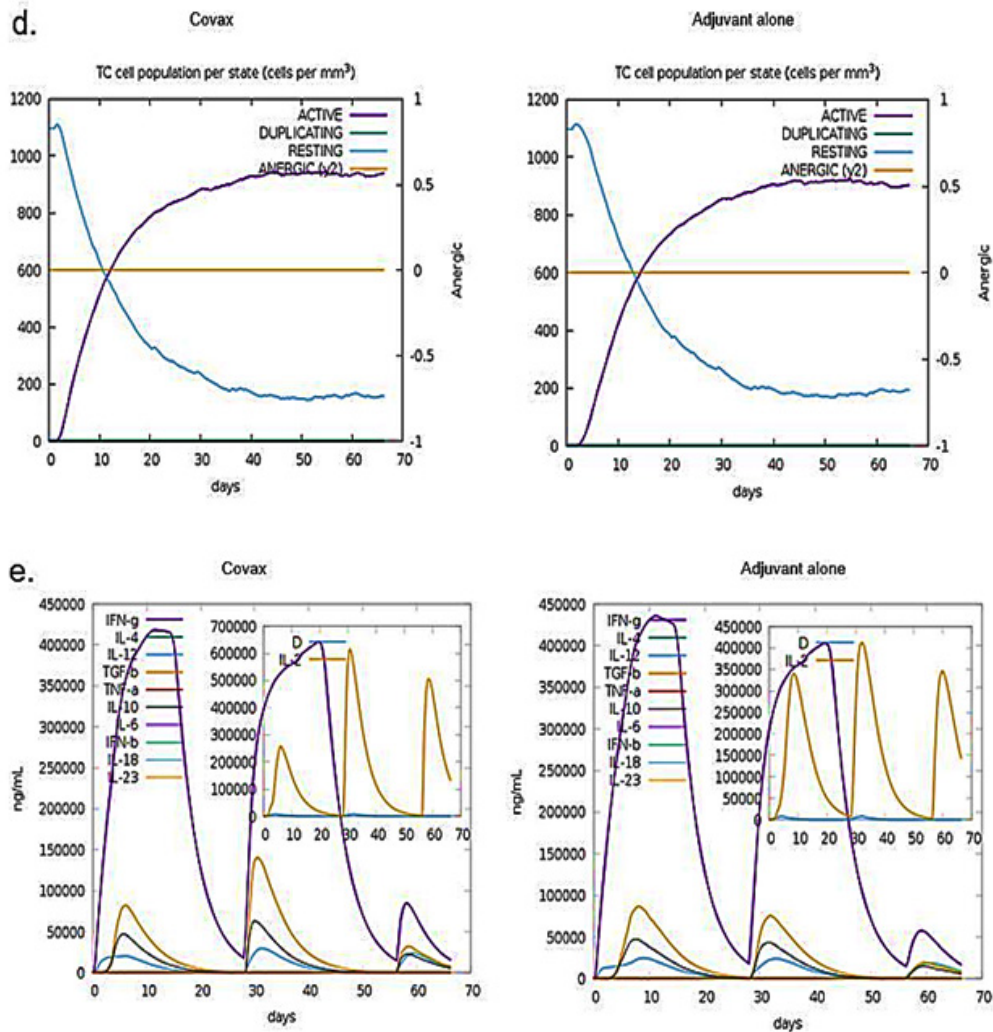


Fig. 5. C-ImmSim simulation profile with Covax and adjuvant (50S RP) alone induced by 3 injections given 4 weeks apart. (a) Immunoglobulin production in response to antigen injections are indicated by black peaks while specific subclasses are indicated by coloured peaks; (b) development of BL populations per isotype; (c) HTL memory and not memory populations; (d) CTL populations per state indicate cell at the resting state not presented with the antigen while the anergic state represents tolerance of the T-cells to the antigen due to repeated exposures; and (e) types of cytokines and interleukins induced wherein the insert plot shows IL-2 level with the Simpson index, D (diversity) indicated by the dotted line. Its value is directly proportional to the emergence of diverse epitope-specific dominant clones of T-cells over time

Results from C-ImmSim simulation showed that Covax can induce potent immune responses. To prove that the generated immune response is not just because of the presence of 50S RP in Covax but also because the multi-epitopes included in Covax can elicit immunogenic response, immune response from Covax was compared versus the adjuvant alone. The primary response is higher as marked by higher levels of IgM with

Covax than with the adjuvant solely (Figure 5a). The secondary and tertiary responses are greater with Covax as indicated by higher memory BL populations (Fig. 5b); and IgG1 + IgG2, IgM, and IgG + IgM levels (Figure 5a). Notice that this trend is also evident with higher HTL (Fig. 5c), and CTL (Fig. 5d) populations for Covax than when adjuvant is used alone. Cytokine and interleukin production are also indicators of successful immune response

from vaccination. Figure 5e shows that Covax induced higher levels of IFN- α , TGF- β , and IL-2 which are important in co-stimulatory signaling for T-cell activation.

In Silico Cloning and Optimization of Covax

The CAI-value for the optimized codons of Covax is 0.95 which is very close to 1. The GC-content, 56.14% is within the optimal range (30%-70%). These results convey that the optimized codons of Covax(1530bp) can be highly expressed in *E.coli* K12 strain as a host.

DISCUSSION

SARS-CoV-2 has higher transmission rate compared with other deadlier coronaviruses, SARS-CoV, and MERS-CoV (Petrosillo *et al.*, 2020). Though it has lower case fatality rate (2.3%), its casualties can be further magnified by its highly contagious nature. Development of vaccines, anti-viral drugs and studies on biological properties of SARS-CoV-2 have been the main focus of researchers around the world since the emergence of COVID-19 pandemic. The most common practices for the prevention of disease-causing viral infections include the use of live attenuated, whole inactivated, or purified antigen. Live attenuated vaccines are often immunogenic; however, some live attenuated vaccines have high risk of virulent virus reversion especially in immunosuppressed individuals. Inactivated vaccines consist of whole or purified antigens, contain components that may cause unwanted adverse effects and tolerability concerns (O'Hagan *et al.*, 2001). The rapid increase in the number of SARS-CoV-2-infected individuals worldwide warrants the development of effective measures to counteract its infection in an accelerated manner. Epitope-based vaccines has gained attention as it offers more potential advantages over whole purified antigen. This approach focuses the immune responses on specific antigenic determinants recognized by immune receptors of lymphocytes while minimizing the undesirable immune reactions from the whole antigen. With the advancements in immunoinformatics, in silico approach is currently employed to successfully discover multi-epitope vaccines against various pathogens (Oli *et al.*, 2020).

Because of their expression abundance,

important roles in viral pathogenesis and replication, all the structural proteins of SARS-CoV-2 were utilized for the screening of epitopes in this work. The protocol used in this study generated 9 linear BL epitopes which are all from S protein. Two antigenic epitopes GFNCYFPLQSYGFQ (485-498) and YGFQPTNGVGYQ (495-506) overlap with the receptor binding motif (RBM) (437-508) site of S protein. RBM is a region in the S protein which binds to angiotensin converting enzyme 2 (ACE2) receptor of the host cell (Letko *et al.*, 2020). Upon binding of antibodies to these epitopes on RBM, the attachment of SARS-CoV-2 to the host cell can be hindered. Studies showed that antibodies are short-lived in convalescent patients compared to HTL and CTL responses which can provide long-term immunity even after a decade of SARS-CoV infection (Channappanavar *et al.*, 2014). Thus, besides linear BL epitopes, T-cell epitopes were also included in the vaccine construct. Activation of BL using epitope-based vaccines requires presentation of MHCII-peptide complex to an activated HTL. One of the major challenges in the development of peptide vaccines is the MHC haplotype-restricted antigen recognition. Thus, this work generated 12 HTL and 12 CTL epitopes with good binding affinity towards the most frequent MHC II and MHC I alleles to cover a large population. A total of 33 epitopes which consist of 9 BL (12-14 residues), 12 HTL (11 residues), and 12 CTL (9-11 residues) epitopes were generated using this protocol. Generally, MHC I molecules bind to peptides with 9-11 residues while MHC II-bound peptides vary from 9-22 residues (Sanchez-Trincado *et al.* 2017). The approach of this work increases the chance of peptide presentation as all four structural antigens have corresponding HTL and CTL epitopes. Even prior to the incorporation of epitopes in the multi-epitope construct, in silico analysis classified all epitopes included in the vaccine as non-allergen which reduces potential allergic reactions. The E-values of epitopes blasted against human protein databases are greater than 1. Matches with E-values smaller than $1.0E-30$ can be cross-reactive in some allergic individuals (Hileman *et al.*, 2002). Thus, these epitopes are less likely to cause autoimmune reactions in humans. Given that all selected epitopes are included in the vaccine, results showed large world population coverage estimated for the set

of HTL (81.81%) and CTL (85.87%) epitopes as well as in areas where infection rates are high. Since some MHC alleles for the sets of HTL and CTL epitopes were not covered by IEDB-PC tool, the estimated population coverage is minimum—the actual percentage can be larger. Having > 80% population coverage, this candidate vaccine may provide herd immunity against SARS-CoV-2 in many populations around the world. In addition, cross-reactivity analysis with 7 HCoV-229E showed that several HTL epitopes IPFAMQMAYRF (S), VTLLAILTALRL (E), SFRLFARTRSM (M), and ALLLLDRLNQL (N); and CTL epitopes QWNLVIGFLF (M), FARTRSMWSF (M), AQFAPSASAF (N), and IPFAMQMAYRF (S) shared 100% sequence identity with SARS-CoV-2 which may offer cross-protection against this virus besides COVID-19.

The form and stability of vaccines are important factors to be considered to ensure efficient delivery of targeted actions. This work focused on developing a multi-epitope vaccine over the use of single epitopes. Advantages include simultaneous induction of immune response as a result of adjoined promiscuous epitopes, linked adjuvant, and exclusion of sequences that may cause unwanted effects. Epitopes were adjoined using AAY and GPGPG linkers which were proven to present sufficient epitopes *in vivo* (Jin *et al.*, 2009; Negahdaripour *et al.*, 2018). While EAAAK linker was used to preserve the bioactivity of adjuvant in Covax (Arai *et al.*, 2001). Incorporating adjuvants in vaccines is essential to be able to enhance its immunogenicity (Lei *et al.*, 2019). This work adjoined the multi-epitopes with 50S RP from *M. Tuberculosis* as an adjuvant since it has been known to bind and activate TLR4. Studies showed that 50S RP induces increased expression of dendritic cell maturation markers, T-cell activation, and cytokines in a TLR4-dependent manner (Lee *et al.*, 2014; Kim *et al.*, 2012). The evaluation of antigenicity and allergenicity of Covax construct classified it as antigenic and non-allergenic, emphasizing its potential and safety as an immunotherapeutic agent. To add to its safety profile, BlastP analysis showed that Covax has no significant matches across human protein databases, avoiding possible autoimmune reactions. *In silico* evaluations of the physicochemical properties of Covax proved its stability. Protein

degradation is often estimated in its amino-terminal residue; thus, Valine was added at the N-terminus of the construct improving its half-life from 30 hours (without Val) to 100 hours (with Val) in mammalian reticulocytes. In addition, the instability index of this candidate vaccine is <40 which implies longer protein half-life *in vivo* based on its dipeptide composition (Guruprasad *et al.*, 1990).

The antigenicity of BL epitopes in a vaccine may also depend on whether they are exposed in the structure of the vaccine so BCRs can easily interact. Results showed that the secondary structures of the series of linear BL epitopes in Covax (337-510) are random coils and extended strands. These epitopes are also found within the disordered regions of the vaccine. Disordered regions in proteins have less tendency to form stable folded structures and are more flexible; therefore, these BL epitopes are more exposed for the binding of BCRs. Several indicators validated the quality of tertiary structures used in this work. Based from the study of Singh and colleagues (2016), any modelled structure exhibiting ERRAT score value > 50 is considered good. In Ramachandran plot analysis, a model with good quality is expected to have at least 90% of residues within the most favored region (Laskowski *et al.*, 1993). Good structures have at least 80% of residues with 3D-1D score > 0.2 (Eisenberg *et al.*, 1997). Evaluations using these quality indicators showed that the improved quality of refined structures versus initial structures justified the need for refinement. These quality indicators also validated the tertiary structure models used for Covax, 50S RP and TLR4 in this study.

The antigenicity of this candidate vaccine is further supported by the resulting linear and discontinuous structural BL epitopes in Covax based from the results in Ellipro. And to prove not just the antigenicity but also immunogenicity, data-driven docking was conducted to determine possible immune interaction between the vaccine and TLR4. This immune receptor was used in the analysis because Covax contains 50S RP which is a known TLR4-agonist. Knowing that 50S RP binds to TLR4 *in vivo*, the values of the binding parameters for 50SRP-TLR4 complex can be used as a control. Results from this work showed that the binding energy and binding affinity of Covax-TLR4, is very close to that of 50SRP-

TLR4. These values also indicate that the binding of Covax to TLR4 is spontaneous (negative ΔG) and that the formation of Covax-TLR4 complex is favoured ($K_d \ll 1$), similar to that of TLR4 with 50S RP alone. Because 50S RP is known to interact with TLR4 *in vivo*; therefore, Covax is expected to interact with TLR4 on immune cells, such as dendritic cells, resulting to development of protective immune response against SARS-CoV-2.

The methods and tools used to select CTL and HTL epitopes were further validated by docking peptides having the lowest binding affinity (highest IC₅₀) with their corresponding MHC alleles. Calculated binding affinities from Prodigy server (K_d) indicate that the binding of each epitope with its MHC allele is favored ($K_d < 1$) and that the formation of HLA-DRB1*04:05-TLLALHRSYLT and HLA-B*53:01-FARTRSMWSF complexes are spontaneous and stable as indicated by negative ΔG values. This step provided more compelling evidence on the accuracy of the T cell prediction methods used in this work—if the tested peptides with the lowest binding affinities (highest IC₅₀) can bind favourably and stably with their corresponding MHC alleles, more so those epitopes in the list with higher binding affinities (lower IC₅₀).

Immune simulation plots for Covax showed that it can induce immune responses. Notice that the levels of IgG, IgM antibodies, memory BL, memory HTL and activated CTL are induced, supporting evident humoral responses and long-term memory persistence after three times exposure with the candidate vaccine. The induced immunogenicity is also evident in the efficacy of antigen clearance from the subsequent injections of the vaccine. Cytokine simulation plot showed increased IFN α and IL-2 with Covax similar to the clinical features observed in SARS-CoV-2-infected patients (Huang *et al.*, 2020). More importantly, the immune responses with Covax is higher than with 50S RP adjuvant alone (Fig.5). For example, the level of primary response IgM antibody titer for Covax (100,000) is much greater than with the adjuvant alone (60,000) (Fig.5a). Notice that IFN- α is highly maintained throughout exposure with Covax but was reduced over time with the exposure to adjuvant alone (Fig.5e). With this comparison, it is evident that the generated immune responses are not just because of the presence of 50S RP in Covax but also because the multi-epitopes

incorporated in Covax (BL, HTL & CTL) can elicit immunogenic responses. The GC content and high codon adaptability index of the optimized codons for Covax recombinant vaccine suggest favorable high level expression in *E. coli* (strain K12).

Results of this work on the potential immunogenicity and safety of Covax were all generated *in silico*. Further studies on the immunogenicity, efficacy, and possible adverse effects should be conducted both *in vitro*, and *in vivo*. Future studies could include the expression of this candidate vaccine in bacterial system to screen for immunoreactivity through serological analysis.

CONCLUSION

Immunoinformatics approach can aid in designing safe and effective prophylactic agents with lesser time required for situations such as COVID-19 pandemic. This is the first work to design a vaccine containing multi-epitopes against all the structural proteins of SARS-CoV-2. Results showed that Covax confers stability, safety and contains epitopes that are antigenic, and immunogenic. Nonetheless, the application of Covax as a candidate vaccine is anticipated to be authenticated both *in vitro* and *in vivo*.

ACKNOWLEDGEMENT

I would like to thank the reviewers who shared helpful insights to this manuscript.

Conflict of interest

I have no conflicts of interest to declare.

Funding source

This work is self-funded.

Research Involving Human Participants/Animals

This article does not contain any work conducted by the author with animals and any human participants.

REFERENCES

1. Ahmed SF, Quadeer AA, McKay MR. Preliminary identification of potential vaccine targets for the COVID-19 coronavirus (SARS-CoV-2) based on SARS-CoV immunological studies. *Viruses*, 12(3): 254 (2020).
2. Al-Tawfiq JA, Zumla A, Memish ZA. Travel implications of emerging coronaviruses: SARS

- and MERS-CoV. *Travel Medicine and Infectious Disease*, **12**(5): 422–428 (2014).
3. Arai R, Ueda H, Kitayama A, *et al.* Design of the linkers which effectively separate domains of a bifunctional fusion protein. *Protein Eng.*, **14**: 529-32 (2001).
 4. Baldazzi V, Castiglione F, Bernaschi M. An enhanced agent based model of the immune system response. *Cell Immunol.*, **244**: 77-79 (2006).
 5. Bui HH, Sidney J, Dinh K, Southwood S, Newman MJ, Sette A. Predicting population coverage of T-cell epitope-based diagnostics and vaccines. *BMC Bioinformatics*, **7**: 153 (2006).
 6. Castiglione F, Duca K, Jarrah A, *et al.* Simulating Epstein–Barr virus infection with C-ImmSim. *Bioinformatics*, **23**: 1371-1377 (2007a).
 7. Castiglione F, Pappalardo F, Bernaschi M, Motta S. Optimization of HAART with genetic algorithms and agent-based models of HIV infection. *Bioinformatics*, **23**: 3350-3355 (2007b).
 8. Channappanavar R, Fett C, Zhao J, Meyerholz DK, Perlman S. Virus-specific memory CD8 T cells provide substantial protection from lethal severe acute respiratory syndrome coronavirus infection. *J Virol.*, **88**(19): 11034-44 (2014).
 9. Colovos C and Yeates TO. Verification of protein structures: patterns of nonbonded atomic interactions. *Protein Sci.*, **2**: 1511-9 (1993).
 10. Dimitrov I, Naneva L, Doytchinova I, *et al.* AllergenFP: allergenicity prediction by descriptor fingerprints. *Bioinformatics*, **30**: 846-51 (2014).
 11. Doytchinova IA and Flower DR. VaxiJen: a server for prediction of protective antigens, tumour antigens and subunit vaccines. *BMC Bioinformatics.*, **8**: 4 (2007).
 12. Eisenberg D, Lüthy R, Bowie JU. VERIFY3D: assessment of protein models with three-dimensional profiles. *Methods Enzymol.*, **277**: 396 404 (1997).
 13. Emini EA, Hughes JV, Perlow DS, *et al.* Induction of hepatitis A virus-neutralizing antibody by a virus-specific synthetic peptide. *J Virol.*, **55**: 836-9 (1985).
 14. Galbadage T, Peterson B, Gunasekera R. Does COVID-19 Spread Through Droplets Alone? *Frontiers in Public Health*, **8**: 163 (2020).
 15. Greenbaum J, Sidney J, Chung J, *et al.* Functional classification of class II human leukocyte antigen (HLA) molecules reveals seven different supertypes and a surprising degree of repertoire sharing across supertypes. *Immunogenetics*, **63**: 325-35 (2011).
 16. Grote A, Hiller K, Scheer M, *et al.* JCat: a novel tool to adapt codon usage of a target gene to its potential expression host. *Nucleic Acids Res.*, **33**: W526-31 (2005).
 17. Guruprasad K, Reddy BV, Pandit MW, *et al.* Correlation between stability of a protein and its dipeptide composition: a novel approach for predicting in vivo stability of a protein from its primary sequence. *Protein Eng.*, **4**: 155-61 (1990).
 18. Hileman RE, Silvanovich A, Goodman RE, *et al.* Bioinformatic methods for allergenicity assessment using a comprehensive allergen database. *Int. Arch. Allergy Immunol.*, **128**: 280–291 (2002).
 19. Hoffmann M, Kleine-Weber H, Schroeder S, *et al.* SARS-CoV-2 Cell Entry Depends on ACE2 and TMPRSS2 and Is Blocked by a Clinically Proven Protease Inhibitor. *Cell*, **181**(2): 271-280 (2020).
 20. Hoof I, Peters B, Sidney J, *et al.* NetMHCpan, a method for MHC class I binding prediction beyond humans. *Immunogenetics*, **61**(1): 1 13 (2009).
 21. Hu Y, Wen J, Tang L, *et al.* The M protein of SARS-CoV: basic structural and immunological properties. *Genomics Proteomics Bioinformatics*, **1**(2): 118 130 (2003). doi:10.1016/s1672-0229(03)01016-7.
 22. Huang C, Wang Y, Li X, *et al.* Clinical features of patients infected with 2019 novel coronavirus in Wuhan, China. *Lancet*, **395**(10223): 497-506 (2020).
 23. Jensen KK, Andreatta M, Marcatili P, *et al.* Improved methods for predicting peptide binding affinity to MHC class II molecules. *Immunology*, **154**(3):394 406 (2018).
 24. Jespersen MC, Peters B, Nielsen M, Marcatili P. BepiPred-2.0: improving sequence-based B-cell epitope prediction using conformational epitopes. *Nucleic Acids Research*, **45**(W1): W24–9 (2017).
 25. Jin X, Newman MJ, De-Rosa S, *et al.* A novel HIV T helper epitope-based vaccine elicits cytokine-secreting HIV-specific CD4+ T cells in a Phase I clinical trial in HIV-uninfected adults. *Vaccine*, **27**: 7080-6 (2009).
 26. Kim K, Sohn H, Kim J-S, *et al.* Mycobacterium tuberculosis Rv0652 stimulates production of tumour necrosis factor and monocytes chemoattractant protein-1 in macrophages through the Toll-like receptor 4 pathway. *Immunology*, **136**(2): 231–240 (2012).
 27. Ko J, Park H, Seok C. GalaxyTBM: template-based modeling by building a reliable core and refining unreliable local regions. *BMC Bioinformatics*, **13**: 198 (2012).

28. Kolaskar AS and Tongaonkar PC. A semi-empirical method for prediction of antigenic determinants on protein antigens. *FEBS Lett.*, **276**: 172-4 (1990).
29. Kozakov D, Hall DR, Xia B, *et al.* The ClusPro web server for protein-protein docking. *Nature Protocols*, **12**(2): 255-278 (2017).
30. Kuo L, Koetzner CA, Masters PS. A key role for the carboxy-terminal tail of the murine coronavirus nucleocapsid protein in coordination of genome packaging. *Virology*, **494**: 100-107 (2016).
31. Laskowski RA, MacArthur MW, Moss DS, *et al.* PROCHECK: a program to check the stereochemical quality of protein structures. *Journal of Applied Crystallography*, **26**: 283-91 (1993).
32. Lee SJ, Shin SJ, Lee MH, *et al.* A potential protein adjuvant derived from *Mycobacterium tuberculosis* Rv0652 enhances dendritic cell-based tumor immunotherapy. *PLoS ONE*, **9**: e104351 (2014).
33. Lei Y, Zhao F, Shao J, *et al.* Application of built-in adjuvants for epitope-based vaccines. *PeerJ*, **6**: e6185 (2019).
34. Letko M, Marzi A, Munster V. Functional assessment of cell entry and receptor usage for SARS-CoV-2 and other lineage B betacoronaviruses. *Nat Microbiol*, **5**(4): 562-569 (2020).
35. Li CK, Wu H, Yan H, *et al.* T cell responses to whole SARS coronavirus in humans. *J Immunol*, **181**(8): 5490-500 (2008).
36. Li Q, Guan X, Wu P, *et al.* Early Transmission Dynamics in Wuhan, China, of Novel Coronavirus-Infected Pneumonia. *N Engl J Med*, **382**: 1199-1207 (2020).
37. Ma Y, Tong X, Xu X, Li X, Lou Z, Rao Z. Structures of the N- and C-terminal domains of MHV-A59 nucleocapsid protein corroborate a conserved RNA-protein binding mechanism in coronavirus. *Protein Cell*, **1**(7): 688-697 (2010).
38. McBride R, van Zyl M, Fielding BC. The coronavirus nucleocapsid is a multifunctional protein. *Viruses*, **6**(8): 2991-3018 (2014).
39. Negahdaripour M, Nezafat N, Eslami M, *et al.* Structural vaccinology considerations for in silico designing of a multi-epitope vaccine. *Infect. Genet. Evol.*, **58**: 96-109 (2018).
40. Neuman BW, Kiss G, Kunding AH, *et al.* A structural analysis of M protein in coronavirus assembly and morphology. *J Struct Biol*, **174**: 11-22 (2010).
41. Nieto-Torres JL, De Diego ML, Verdiá-Báguena C, *et al.* Severe acute respiratory syndrome coronavirus envelope protein ion channel activity promotes virus fitness and pathogenesis. *PloS Pathog*, **10**(5): e1004077 (2014).
42. O'Hagan DT, MacKichan ML, Singh M. Recent developments in adjuvants for vaccines against infectious diseases. *Biomol Eng*, **18**: 69-85 (2001).
43. Oli AN, Obialor WO, Ifeanyichukwu MO, *et al.* Immunoinformatics and Vaccine Development: An Overview. *Immunotargets Ther*, **9**: 13-30 (2020).
44. Oyarzún P, Kobe B. Recombinant and epitope-based vaccines on the road to the market and implications for vaccine design and production. *Human Vaccines & Immunotherapeutics*, **12**(3):763-767 (2016).
45. Pan M, Wang X, Liao J, *et al.* Prediction and identification of potential immunodominant epitopes in glycoproteins B, C, E, G, and I of herpes simplex virus type 2. *Clinical & Developmental Immunology*, 2012: 205313 (2012).
46. Petrosillo N, Viceconte G, Ergonul O, Ippolito G, Petersen E. COVID-19, SARS and MERS: are they closely related?. *Clin Microbiol Infect*, **26**(6): 729-734 (2020).
47. Pleguezuelos O, James E, Fernandez A, *et al.* Efficacy of FLU-v, a broad-spectrum influenza vaccine, in a randomized phase IIb human influenza challenge study. *NPJ Vaccines*, **5**: 22 (2020).
48. Ponomarenko J, Bui H, Li W, *et al.* ElliPro: a new structure-based tool for the prediction of antibody epitopes. *BMC Bioinformatics*, **9**: 514 (2008).
49. Rapin N, Lund O, Bernaschi M, Castiglione F, *et al.* Computational Immunology Meets Bioinformatics: The Use of Prediction Tools for Molecular Binding in the Simulation of the Immune System. *PLoS ONE*, **5**(4): e9862 (2010).
50. Saha Sand Raghava GP. Prediction of continuous B-cell epitopes in an antigen using recurrent neural network. *Proteins*, **65**: 40-8 (2006).
51. Sanchez-Trincado JL, Gomez-Perosanz M, Reche PA. Fundamentals and Methods for T- and B-Cell Epitope Prediction. *J Immunol Res*, 2017:2680160 (2017).
52. Shannon C. The mathematical theory of communication. *Bell Syst Tech J*, **27**: 379-423 (1948).
53. Singh S., Singh D.B., Singh A., Ram B.G.G., Dwivedi S., Ramteke P.W. An approach for identification of novel drug targets in *Streptococcus pyogenes* SF370 through pathway analysis. *Interdiscip. Sci. Comput. Life Sci*, **8**: 388-394 (2016).
54. Vaishnav N, Gupta A, Paul S, John GJ. Overview of computational vaccinology: vaccine

- development through information technology. *J Appl Genet*, **56**(3):381-391 (2015).
55. Verdia-Baguena C, Nieto-Torres JL, Alcaraz A, Dediego ML, Enjuanes L, Aguilera VM. Analysis of SARS-CoV E protein ion channel activity by tuning the protein and lipid charge. *Biochim Biophys Acta*, **1828**: 2026–2031 (2013).
56. Walls AC, Tortorici MA, Bosch BJ, *et al.* Cryo-electron microscopy structure of a coronavirus spike glycoprotein trimer. *Nature*, **531**(7592):114-117 (2016).
57. Wang D, Hu B, Hu C, *et al.* Clinical Characteristics of 138 Hospitalized Patients With 2019 Novel Coronavirus-Infected Pneumonia in Wuhan, China. *JAMA*, **323**(11): 1061–1069 (2020).
58. Weiskopf D, Angelo MA, de Azeredo EL, *et al.* Comprehensive analysis of dengue virus-specific responses supports an HLA-linked protective role for CD8+ T cells. *Proc Natl AcadSci U S A*, **110**(22): E2046-E2053 (2013).
59. Wilson L, McKinlay C, Gage P, Ewart G. SARS coronavirus E protein forms cation-selective ion channels. *Virology*, **330**: 322–331 (2004).
60. Xue LC, Rodrigues JP, Kastritis PL, Bonvin AM, Vangone A. PRODIGY: a web server for predicting the binding affinity of protein-protein complexes. *Bioinformatics*, **32**(23) :3676-3678 (2016).
61. Zhou P, Yang XL, Wang XG, *et al.* A pneumonia outbreak associated with a new coronavirus of probable bat origin. *Nature*, **579**(7798): 270-273 (2020).
62. Zhu X, Liu Q, Du L, Lu L, Jiang S. Receptor-binding domain as a target for developing SARS vaccines. *J Thorac Dis.*, **5** Suppl 2(Suppl 2): S142-S148 (2013).